Published online: 2020-02-21

Bimodal ERCP, a new way of seeing things

OPEN ACCESS

Authors

Marcus Reuterwall[1,2], Alexander Waldthaler[1,3], Jeanne Lubbe[1,4], Nils Kadesjö[5], Raffaella Pozzi Mucelli[1,6], Marco Del Chiaro[1], Matthias Lohr[1], Urban Arnelo[1,3]

Institutions

1 Karolinska Institute, CLINTEC, Stockholm, Sweden
2 Ersta Hospital – Surgery, Stockholm, Sweden
3 Karolinska University Hospital – Upper Abdominal Diseases, Stockholm, Sweden
4 University Stellenbosch – Division of Surgery, Stellenbosch, Western Cape, South Africa
5 Karolinska University Hospital – Medical Radiation and Physics and Nuclear Medicine, Stockholm, Sweden
6 Karolinska University Hospital – Abdominal Radiology, Stockholm, Sweden

submitted 26.6.2019
accepted after revision 4.11.2019

Bibliography
DOI https://doi.org/10.1055/a-1070-8749 |
Endoscopy International Open 2020; 08: E368–E376
© Georg Thieme Verlag KG Stuttgart · New York
eISSN 2196-9736

Corresponding author
Marcus Reuterwall, CLINTEC, Karolinska Universitetssjukhuset, K56 Huddinge, 14186 Stockholm, Sweden
Marcus.reuterwall.hansson@ki.se

ABSTRACT

Background and study aims Conventional endoscopic retrograde cholangiopancreatography (ERCP) is hampered by two-dimensional visualization, post-procedural adverse events (AEs), and exposure to ionizing radiation. Bimodal ERCP might mitigate these challenges, but no reports of its use are available to date. The aim of this study was to explore the feasibility of bimodal ERCP, while investigating its potential clinical yield.

Patients and methods This was a retrospective observational study of patients that underwent bimodal ERCP in a single tertiary academic referral center. Thirteen patients undergoing conventional ERCP had a previously T2-weighted isotropic 3 D TSE MRCP sequence aligned and fused with the two-dimensional image generated from the fluoroscopy c-arm unit in real time.

Results Over a 2-month period, 13 patients with a mean age of 54 underwent bimodal ERCP for bile duct stricture (61.5 %), complex cholelithiasis (7.7 %) and ductal leakage (30.1 %). Bimodal ERCP was feasible in all 13 cases, and image quality was assessed as "good" in 11 patients (84.6 %). Bimodal ERCP aided in visualizing the lesion of interest (76.9 %), assisted in understanding the 3 D anatomy of the biliopancreatic ductal system (61.5 %), and aided in finding a favorable position for the c-arm (38.4 %) for subsequent therapeutic intervention.

Conclusions This first report on bimodal ERCP proves its feasibility and suggests that it may assist in increasing both the diagnostic and therapeutic yield of ERCP, while at the same time decreasing AEs during and after ERCP. Its main application might lie in treatment of complex intrahepatic disease.

Introduction

Biliary diagnostics and therapeutics are evolving as technology advances. Magnetic resonance imaging (MRI) allows for detailed three-dimensional (3 D) biliary anatomical reconstruction, while sparing the patient ionizing radiation and iodinated contrast medium exposure. It has become the investigation of choice for non-invasive diagnosis of biliary pathology [1–4]. Although endoscopic retrograde cholangiopancreatography (ERCP) carries a 5 % to 10 % risk of adverse events (AEs), it allows for tissue acquisition and therapeutic intervention, often obviating the need for more invasive options. It has been established as the minimally invasive access of choice when considering biliary intervention in many instances [5–7].

Conventional ERCP is guided by two-dimensional (2 D) fluoroscopic images where contrast-filled ducts become visible, but it is limited in several ways. It renders the endoscopist "blind" to both subtle periductal soft tissue pathology, as well as ductal systems upstream to tight strictures not allowing for contrast passage [8]. In patients with clearly undrained intrahepatic segments after conventional ERCP, cholangitis has been reported in up to 8.8 % to 16.6 % of cases [9–11]. In addition, ionizing radiation risks to both patients and to personnel are well described [12].

▶ **Table 1** Technical parameters of the MRI examinations.

Sequence	Plane	Slice thickness/gap	Te (ms)	Tr (ms)	Breathing technique	Scan time
T2w-HASTE	axial	4 mm/0	76.0	1000	Multi-BH[1]/PACE[2]	2–5 min
T2w-HASTE	coronal	4 mm/0	76.0	1000	PACE	2–5 min
T1w 3 D GRE Dixon	axial	4 mm/0	2.4–4.8	6.93	BH	15–22 s
T2w 3D-SPACE MRCP	coronal	1 mm	900.0	2000	PACE	3–6 min
DWI[3]	axial	5 mm/0	77.0	5000	FB[4]	3–5 min
T1w 3D-GRE VIBE FS before contrast	axial	2,5 mm	1.9	4.29	BH	15–22 s
T1w 3D-GRE VIBE FS after contrast[5]	axial	2,5 mm	1.9	4.29	BH	5 min

[1] BH, breath-hold
[2] PACE, prospective acquisition correction navigator-triggered
[3] DWI was acquired with the following b-values: 50 and 800 s/mm^2
[4] FB, free-breathing
[5] The following dynamic phases were acquired: late arterial phase by means of the Combined Applications to Reduce Exposure (CARE) bolus technique; portal venous phase, acquired with a delay of 50 seconds from the start of the arterial phase; delayed phases at 3 and 5 min respectively.

Accessing prior knowledge on patient specific anatomy and pathology at the time of a minimally invasive intervention such as ERCP promises to assist the endoscopist with challenging maneuvers, potentially increasing therapeutic success. The ability to combine pre-procedural computed tomography (CT) images with imaging obtained at the time of intervention has extensively been reported on for other types of image guided interventions, for example endovascular procedures, revealing a clear decrease in procedure time and radiation dose [13–15]. Utilization of pre-procedural MRI images has likewise been described in the setting of aortic endovascular and neurosurgical intervention [16, 17] but to our knowledge, use of bimodal technology at the time of ERCP has not been investigated before. The 3 D diagnostic images obtained during pre-procedural MRI of the biliopancreatic ductal system can be aligned and fused in the sagittal, coronal, and transverse planes with real-time 2 D fluoroscopic images at time of ERCP. This bimodal imaging technique provides real-time guidance via a 3 D roadmap and has the potential of combining the diagnostic value of MRI with the therapeutic advantages of ERCP. The aim of this study was to explore the feasibility of bimodal ERCP, while investigating its potential clinical yield.

Patients and methods

The current study was an observational retrospective study of consecutive patients undergoing bimodal ERCP at a single tertiary referral center. Patients considered for inclusion were those that had a previously planned conventional ERCP at our single tertiary referral center during the study period. Only patients who, in addition, had a previously obtained T2-weighted isotropic 3 D MRI dataset were eligible. Among eligible patients, we selected cases representing a variety of different clinical problems. Before utilizing this technique in a clinical setting, our team underwent a 3-hour image co-registration simulation session under tuition of an application specialist. By making use of both MRI and fluoroscopic images of an inanimate phantom (a water bottle), subsequent fusion and bimodal image creation was accomplished, after which our team could proceed independently. The Swedish Ethical Review Authority approved the study (dnr:2019-02109).

MRI imaging

All MRIs were performed on a 1.5 T system (Magnetom Avanto or Magnetom Aera, Siemens Healthcare, Erlangen, Germany) in combination with a phased-array body and spine matrix coil. The examinations included the following sequences: T2-weighted HASTE on the axial and coronal plane, axial 3 D T1-weighted DIXON, 3 D T2-weighted MRCP coronal images with maximum intensity projection (MIP), axial DWI, axial 3 D T1-weighted fat-sat VIBE before and after intravenous administration of Gadolinium-based contrast agent (0.05 mmol/kg for Gadobenate dimeglumine at an injection rate of 2 mL/s; or 0.025 mmol/kg of Gadoxetic acid at a flow rate of 1 mL/s). Contrast media injections were followed by a bolus of 20 ml saline flush. Technical parameters are summarized in ▶ **Table 1**.

On the day of the ERCP procedure, the MRI examination was imported from the Picture and Archiving Communication System (PACS) from Sectra AB, Linköping, Sweden, into the 3D-workstation by (Siemens Healthcare, Erlangen, Germany) in the intervention suite and reconstructed in 3 D volume-rendering formats.

MRI co-registration and fusion with fluoroscopic image

Under general anesthesia and breath-hold, a frontal and lateral fluoroscopic image of the upper abdomen was obtained in our interventional suite using a roof mounted c-arm system (Artis Q, Siemens Healthcare, Erlangen, Germany) as previously described in detail by Schwein et al [16]. In some cases, single-image digital acquisitions were obtained, since the fluoroscopic images were considered of insufficient image quality. Typically, T1-weighted 3D-GRE VIBE fat-sat sequences were selected for initial image co-registration because of better spatial resolu-

tion, and then replaced by 3D T2-weighted MRCP images where the biliopancreatic ductal system is more visible. The MRI and fluoroscopic images were co-registered using appropriate landmarks visible in both modalities, usually the liver dome and the spine. These landmarks were electronically marked using a dedicated software (syngo iGuide toolbox; Siemens Healthcare, Erlangen, Germany) and co-registered using a dedicated software (syngo Inspace 3D-2D; Siemens Healthcare, Erlangen, Germany), followed by manual alignment of landmarks visible in both image modalities. During bimodal ERCP, the co-registered MRI-derived cholangiopancreatogram (co-MRCP) was projected in real time onto the live conventional fluoroscopic image on the endoscopists monitor. The amount of opacity for each image, namely co-MRCP vs. conventional fluoroscopic, can be manually chosen by the endoscopist. A change in table position and/or x-ray source ("C-arm") angulation, results in automatic adjustment of the co-MRCP on the endoscopist monitor to correspond with the new fluoroscopic view. This image co-registration technology is available on several imaging system irrespective of vendor situation.

The workflow of this fluoroscopy image and co-registration with the preprocedural MRI is illustrated in ▶ **Fig. 1**.

Data collection

Patient demographics included age, sex, American Society of Anesthesiologists (ASA) functional classification, as well as indication for undergoing the procedure. Procedural parameters included time since the preoperative MRI utilized for image co-registration was obtained, and whether bimodal ERCP was technically possible. Qualitative procedural parameters included image quality, aid in visualization, aid in understanding 3D ductal anatomy, and aid in finding c-arm position, and both intra- and extrahepatic overlay misalignment. All qualitative procedural recordings were made by two endoscopists performing and assisting in each procedure. In case of discrepant result, the images were retrospectively reviewed together with a third senior endoscopist and evaluated again in consensus. Overlay misalignment in bimodal image mode was evaluated using a custom developed qualitative assessment scale. Radiation dose data (including the dose area product and fluoroscopy time) and the exposure log for each patient were automatically archived as a Radiation Dose Structured Report (RDSR) DICOM-object. Radiation dose during image co-registration was identified from the C-arm and table movements listed in the exposure log, combined with the total image co-registration time. Total procedure time, image co-registration time, and total amount of contrast medium (240 mg iodine/mL, Omnipaque, GE Healthcare, Little Chalfont, UK) was documented.

Definitions

Bimodal image quality was defined as "good" if the images of the biliopancreatic ductal system from both the co-MRCP and the conventional fluoroscopic images of contrast-filled ducts were clearly visible in bimodal image mode. Bimodal ERCP was assessed as "an aid in visualizing the lesion of interest" if the co-MRCP showed the lesion of interest in bimodal image mode with the conventional fluoroscopic image being native, i. e. not contrast medium enhanced. In one case, the lesion of interest was electronically marked on the preprocedural MRI in consultation with a radiologist, and then this electronic marker was merged with the bimodal image for additional guidance. Bimodal ERCP was defined as "an aid in understanding 3D ductal anatomy" if the co-MRCP provided information about ductal trajectory in the anteroposterior, mediolateral or longitudinal axis not comprehensible with the conventional fluoroscopic image. The absence of overlay misalignment in bimodal image mode was defined as: The guidewire trajectory in a native fluoroscopic image and/or contrast filled ducts visible in conventional unimodal fluoroscopic mode matches the ducts from the co-MRCP perfectly regardless of angle of the c-arm unit.

Statistical analyses

All analyses were carried out using STATA 13.1 (StataCorp LP, College Station, Texas, United States).

Results

Between March 15, 2017 and May 21, 2017, 13 patients with a mean age of 54 (range 22–80) underwent bimodal ERCP at our tertiary endoscopy unit. Ten patients (76.9 %) were male, three (23.1 %) were female, with five (38.5 %) classified as ASA 2 and 8 (61.5 %) as ASA 3. Bile duct stricture was the indication for undergoing ERCP in eight patients (61.5 %) and complex cholelithiasis in one (7.7 %). The cause of biliary strictures ranged from indeterminate stricture in non-PSC patients (n = 4), indeterminate stricture in PSC patients (n = 2), and stricture after liver transplantation (n = 2). Ductal leakage was the indication for ERCP in four patients (30.1 %), and included bile duct (n = 2) as well as pancreatic duct (n = 2) leaks. Average time between the pre-procedural MRI and the bimodal ERCP procedure was 91 days (range 1–240) as depicted in ▶ **Table 2**.

MRI co-registration and fusion with fluoroscopic image was technically possible in all 13 cases, and image quality was assessed as "good" in 11 patients (84.6 %) and "poor" in two (15.4 %). Bimodal ERCP aided in visualizing the lesion of interest in 10 patients (76.9 %). In one patient with PSC and a dominant segmental duct stricture, the co-MRCP visualized the stricture, whereas the conventional fluoroscopic image did not (▶ **Table 3**). Bimodal ERCP assisted in understanding the 3D anatomy of the biliopancreatic ductal system without exposing the patient or health care personnel to radiation in eight patients (61.5 %). In five patients (38.4 %), bimodal ERCP aided in finding a favorable position for the c-arm for subsequent therapeutic intervention with conventional ERCP-technique. This position was found without exposing the patient to additional ionizing radiation while evaluating different angles of view on the co-MRCP. ▶ **Fig. 2** demonstrates examples of image quality in bimodal ERCP.

Overlay misalignment between the co-MRCP and the conventional fluoroscopic image was major in extrahepatic structures in 11 patients (84.2 %), non-applicable in one (7.7 %) and moderate in one (7.7 %). In the non-applicable case, the intrahepatic bile ducts were accessed through a Roux-en Y hepatico-

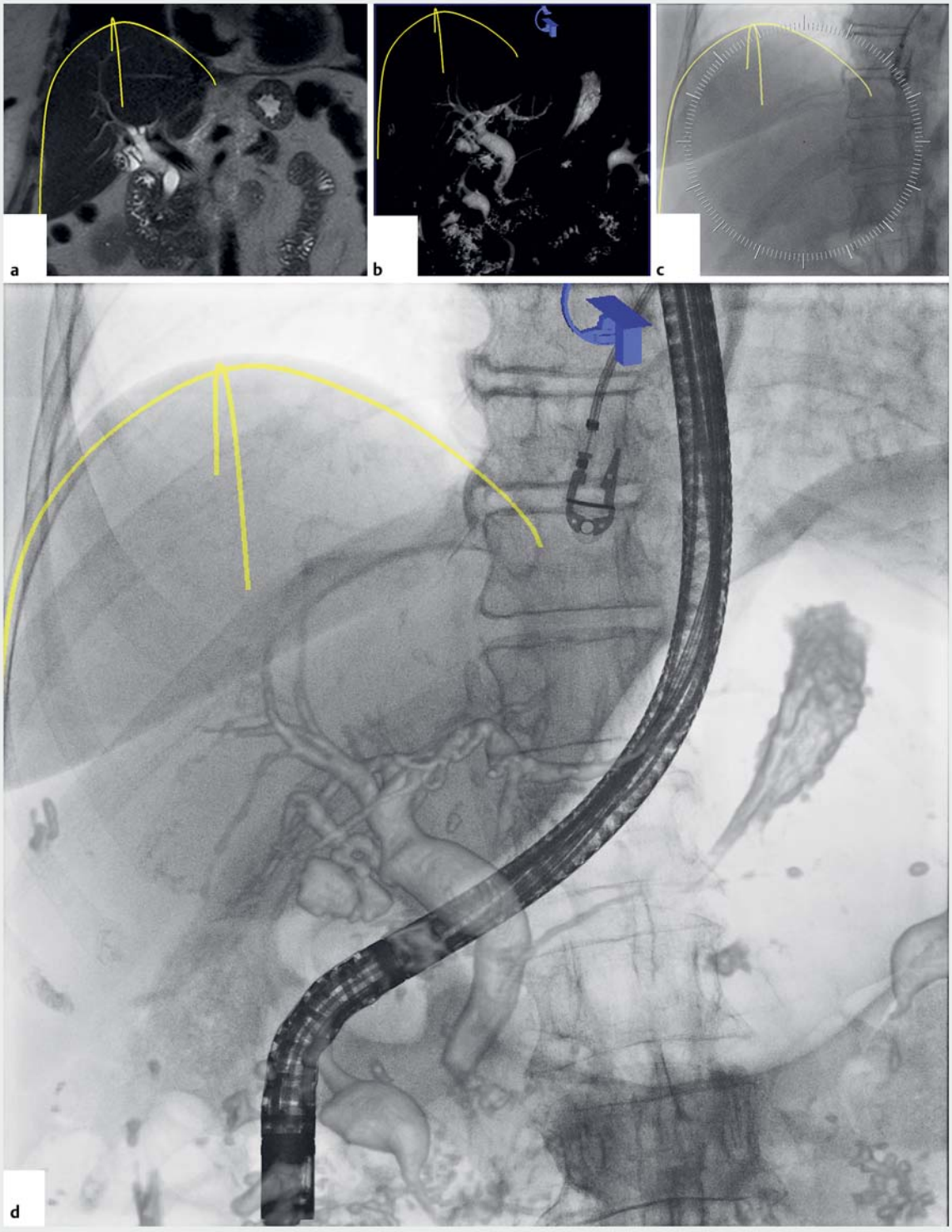

▶ **Fig. 1** Workflow illustrates magnetic resonance imaging (MRI)–conventional fluoroscopy image coregistration and fusion to bimodal ERCP. Preprocedural planning involves marking of landmarks visible in both image modalities in coronar and lateral projections (only coronar projections shown here). **a** The liver contour is marked in T1-weighted 3D-GRE VIBE fat-sat MRI sequence where soft tissues are visible. **b** The initial MRI sequence is replaced by 3 D T2-weighted MRCP images where the biliopancreatic ductal system is better visualized. **c** The liver contour in a standard fluoroscopic image is marked. **d** After manual alignment of landmarks visible in both image modalities, the coregistered and fused bimodal image is projected in real time to the endoscopists monitor for intraprocedural guidance.

▶ **Table 2** Patient demographics, procedure indication, and time between preprocedural MRI and procedure.

Patient	Age, years	ASA	Sex	Indication	Time between pre-procedural MRI and procedure, days
1	77	2	F	Complex cholelithiasis	135
2	73	3	M	Indeterminate biliary stricture(non-PSC)	128
3	79	3	M	Indeterminate biliary stricture(non-PSC)	23
4	80	3	F	Indeterminate biliary stricture (non-PSC)	36
5	22	2	F	Biliary duct leakage	199
6	74	3	M	Postoperative pancreatic duct leakage	1
7	48	3	M	Indeterminate biliary stricture (PSC)	67
8	47	2	M	Indeterminate biliary stricture(non-PSC)	40
9	25	2	M	Biliary duct leakage with disconnected duct	20
10	37	3	M	Bile duct strictures after liver transplantation	56
11	51	3	M	Pancreatic duct leakage	185
12	27	2	M	Indeterminate biliary stricture (PSC)	49
13	60	3	M	Bile duct strictures after liver transplantation	240
Mean	54				91

MRI, magnetic resonance imaging; PSC, primary sclerosing cholangitis

▶ **Table 3** Image quality of bimodal ERCP.

Patient	Bimodal ERCP image quality	Aid in visualize lesion of interest?	Aid in understanding 3 D ductal anatomy?	Aid in finding C-arm position?	Intrahepatic overlay misalignment? (none, +, ++, +++)	Extrahepatic overlay misalignment? (none, +, ++, +++)
1	Good	Yes	No	No	None	+++
2	Good	No	Yes	Yes	+++	+++
3	Good	Yes	No	No	None	+++
4	Good	Yes	Yes	No	None	+++
5	Good	Yes	No	Yes	++	+++
6	Poor	No	No	No	N/A	+++
7	Good	Yes	Yes	No	++	+++
8	Good	No	No	No	++	+++
9	Good	Yes	Yes	No	+	++
10	Poor	Yes	Yes	Yes	None	N/A
11	Good	Yes	Yes	No	N/A	+++
12	Good	Yes	Yes	Yes	+	+++
13	Good	Yes	Yes	Yes	None	+++

Overlay misalignment in bimodal image mode evaluated using a custom-developed qualitative assessment scale: none, minor (+), moderate (++) and major (+++).
ERCP, endoscopic retrograde cholangiopancreatography

jejunostomy. In the two patients where the indication was pancreatic duct leakage, the overlay misalignment between the two images of the main pancreatic duct was major. There was no intrahepatic overlay misalignment in five cases (38.4 %), major misalignment in one (7.7 %), moderate misalignment in three (23.1 %) and minor misalignment in two (15.4 %). In the case with major overlay misalignment in intrahepatic structures, the patient had a stent in the intrahepatic ducts causing

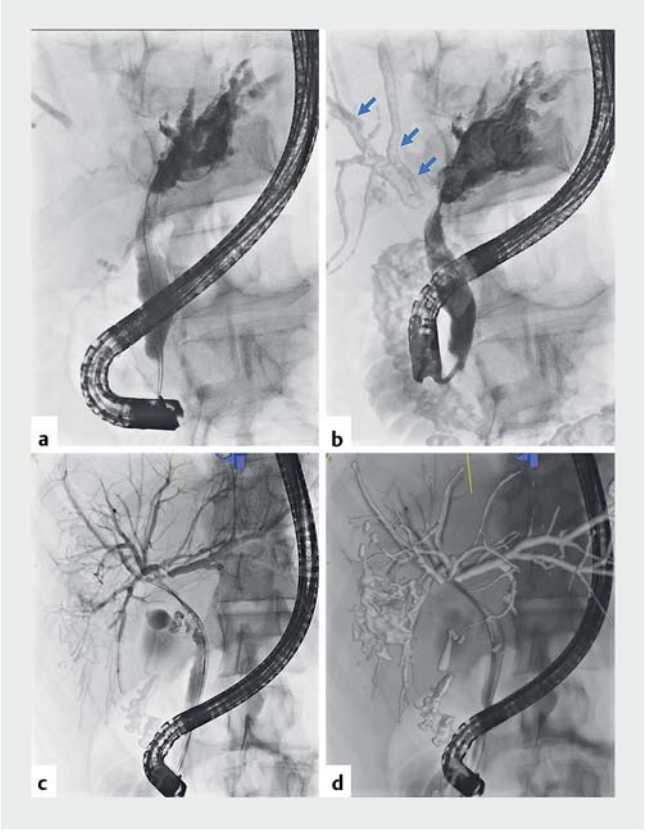

▶ **Fig. 2** Image quality in bimodal ERCP. **a** Conventional fluoroscopic ERCP image in a patient with a narrow hilar stricture. Only a small amount of contrast has reached the right sided central bile ducts which are barely visible. **b** Bimodal ERCP in the same patient as in **a**, where the conventional fluoroscopic image is fused and aligned with a pre-procedural MRCP. In this image mode the right sided ducts are visible (blue arrows) **c** Bimodal ERCP with slight overlay of an aligned and fused MRCP sequence. **d** Bimodal ERCP in same patient as in **c** with increased overlay of an aligned and fused MRCP sequence.

ductal deformation during the MRI investigation which was removed in the initial phase of the bimodal ERCP procedure. Overlay mismatch due to breathing artefacts between the dynamic live images obtained during continuous fluoroscopy and the static co-MRCP were consistent. ▶ **Fig. 3a** and ▶ **Fig. 3b** demonstrate examples of misalignment between the two image modalities.

Total radiation dose for the whole procedure was a mean of 22.7 Gy cm^2 (range 1.5–62.6), and the image registration radiation dose was a mean of 1.12 Gy cm^2 (range 0.17–3.53), as is shown in ▶ **Table 4**. Two cases (patients 8 and 11) had considerably higher image co-registration radiation dose compared to the rest. The co-registration process of these two patients was characterized by long fluoroscopy times and/or use of single image digital acquisitions during the lateral projections. Total procedure time was a mean of 75.7 min (range 22.4–147.6), and time for image co-registration process a mean of 11.9 min (range 5.7–24.7). The time for image co-registration included software malfunction and system reboot in one case. Total amount of contrast medium used throughout the whole procedure was a mean of 55.3 mL (range 6.0–140 mL). No contrast medium was used during the image co-registration process.

Discussion

This study is the first to report on fusion of pre-procedural 3 D MRI images with live 2 D fluoroscopic images at the time of ERCP, combining the advantages of both imaging modalities. The bimodal ERCP technique was technically feasible in all 13 patients, and good bimodal images were obtained in 84.6 %.

To visualize the biliary ductal system during conventional ERCP, the endoscopist uses ionizing radiation while contrast medium is injected to generate fluoroscopic images of the biliary tree. The resulting image provides a 2 D roadmap that guides the procedure, but gives little or no information about 3 D anatomy or non-contrast opacified structures. In the current study real-time access to 3 D MRI images at the time of ERCP, aided in visualization of the lesion of interest in 76.9 % of cases, and aided in understanding ductal anatomy in 61.5 % of cases, while adding minimal radiation exposure and procedure time.

Bimodal ERCP technology was tested for a range of indications during conduction of this study, with bile duct obstruction being the most common (69.2 %). When attempting to traverse an obstruction with a wire in order to facilitate brush cytology and/or stent placement, a 3 D roadmap available at the time of wire manipulation is especially helpful. The ability to visualize both the lateral and anteroposterior position of a duct proximal to a stricture, independent of contrast opacification, allows for maneuvers to manipulate wire advancement in an optimal direction without the risk for cholangitis and adverse effects related to ionizing radiation. In the current report bimodal ERCP aided in understanding ductal anatomy in six of eight patients (75 %) undergoing the procedure for stricture evaluation and treatment.

Diagnostic and surveillance challenges posed by indeterminate biliary strictures, especially in PSC patients, are well known [18, 19]. In the current study, bimodal ERCP unveiled a dominant segmental stricture in a patient with PSC, not otherwise seen on conventional fluoroscopy. Although difficult to assess and analyze, the additional information on periductal soft tissue that bimodal ERCP affords, might be of value in drawing attention to dominant strictures or periductal mass lesions requiring urgent investigation and/or intervention. In patients undergoing ERCP for a ductal leak, upstream contrast opacification might prove impossible, and the ability for bimodal ERCP to “show the way” becomes even more important, as was seen in the single patient reported on with a leak and ductal disconnect.

The concept that a 3 D roadmap might facilitate the diagnostic performance of ERCP, has been explored before [20, 21] albeit with the use of 180° rotation of the c-arm and 3 D image rendering. This technique requires the initial injection of contrast medium to opacify anatomy proximal to the point of obstruction, and necessitates additional ionizing radiation to both patient and health personnel. In the current study, the bimodal image obtained by image fusion, aided in understanding

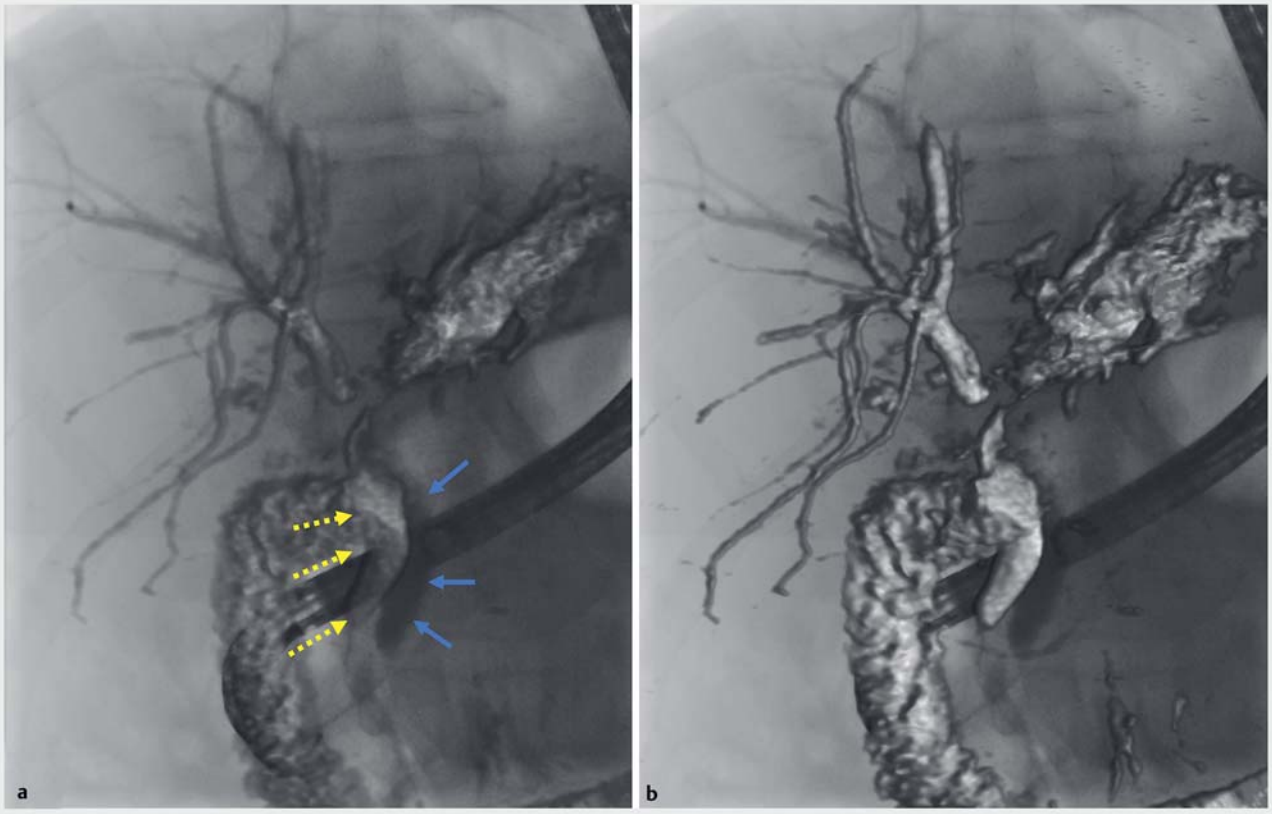

▶ **Fig. 3** Examples of misalignment between the two image modalities. **a** Bimodal ERCP in a patient with a hilar stricture. The image of the extrahepatic bile duct obtained from preprocedural MRCP (dotted yellow arrows) is clearly misaligned with the image of the contrast filled extrahepatic duct obtained from conventional fluoroscopy(blue arrows). In the intrahepatic ducts, there is only minor misalignment. **b** Same patient as in **a**, but with increased overlay of an aligned and fused MRCP sequence.

biliary anatomy and c-arm positioning before intervention, during which time little additional radiation (1.12 Gy cm^2) and no injection of contrast medium was needed. The radiation dose needed for MRI and fluoroscopic image co-registration can be considered negligible or minor compared to the total radiation dose from each procedure (mean 22.7 Gy cm^2). In only 2 cases did the dose from co-registration constitute more than 15 % of the total dose, with the mean being 8 % contribution for all patients. However, with the visual aid of bimodal ERCP, it is likely that less radiation is needed during the rest of the procedure, possibly even resulting in a decrease in total radiation dose. From the current study, it was not possible to estimate this change in radiation dose. Image co-registration could be completed in a mean time of 12 minutes, adding minimally to total procedure time (mean 75.7 minutes).

A limitation of the current study was the limited number of patients reported on, but the main aim of exploring feasibility of bimodal ERCP was confirmed, with 85 % of images regarded as good. Alignment between co-MRCP and ERCP images in the frontal, sagittal, and transverse planes were correct in intrahepatic ducts in 77 % of cases, while less fixed extrahepatic ducts, prone to displacement during the procedure, were frequently misaligned during bimodal ERCP. This held true also for intervention in the pancreatic duct and is likely explained by air insufflation and manipulation of the duodenoscope inside the bowel.

The abundance of diagnostic anatomical and pathological information afforded by MRI can be accessed by the endoscopist at the time of intervention by means of bimodal technology. Image fusion capability is available on several imaging systems irrespective of vendor or provider, and we foresee few challenges during introduction of this technique, also outside of specialized centers. Bimodal ERCP aids in visualization of lesions and understanding of ductal anatomy, possibly increasing technical success rates, and decreasing risk for post-ERCP cholangitis. Bimodal ERCP assists in optimal c-arm positioning and likely decreases total contrast and radiation doses. Its main use may lie in the assessment and endoscopic treatment of complex intrahepatic biliary disease, where overlay misalignment is less of a challenge.

Conclusion

This first report on bimodal ERCP proves the feasibility of accessing the diagnostic value of preprocedural MRI at the time of conventional therapeutic ERCP. Bimodal ERCP can aid in under-

▶ **Table 4** Intraprocedural parameters recording.

Patient	Total radiation dose (Gy cm²)	Image registration radiation dose (Gy cm²)	Fraction of radiation dose from registration (%)	Total fluoro time (min)	Total procedure time (min)	Time image registration process (min)	Total amount contrast medium (mL)
1	6.2	0.32	5%	6.4	35.3	8.1	35.0
2	21.7	0.82	4%	26.4	147.6	14.8	65.0
3	5.6	0.85	15%	8.1	103.1	24.7	20.0
4	11.3	0.36	3%	21.7	95.2	20.1	54.0
5	1.5	0.31	21%	5.7	34.6	10.2	25.0
6	23.3	<2.59[1]	11%	22.7	50.1	10.5	7.0
7	57.5	0.89	2%	35.1	90.2	15.1	62.0
8	21.0	2.95	14%	16.7	25.5	9.8	70.0
9	10.4	0.17	2%	32.6	56.3	7.1	50.0
10	41.7	0.33	1%	37.4	145.1	12.4	130.0
11	14.4	3.53	24%	6.9	22.4	6.8	6.0
12	18.5	0.51	3%	26.3	59.7	5.7	55.0
13	62.6	0.91	1%	49.3	118.7	10.0	140.0
Mean	22.7	1.12	8%	22.7	75.7	11.9	55.3
Max	62.6	3.53	24%	49.3	147.6	24.7	140.0
Min	1.5	0.17	1%	5.7	22.4	5.7	6.0

Radiation dose in the form of dose area product.
[1] The exact period of the fusion process could not be identified in the exposure log. The real image registration dose was less than the listed “worst case”.

standing biliary anatomy, visualizing the area of interest, and positioning of the c-arm. Future larger studies are required to definitively determine whether this new approach can increase the clinical yield and technical success, while at the same time reducing radiation exposure and contrast medium usage during ERCP.

Acknowledgements

A part of this paper was presented at the Digestive Disease Week, May 18–21, 2019 in San Diego, USA (Gastrointestinal Endoscopy. 2019; 89 (Suppl 6): Sa1475) https://doi.org/10.1016/j.gie.2019.03.269. We thank Mr. Yoshinori Takeyama (Honyaku Center Inc., Tokyo) for proofreading and correcting any English language-related issues in this manuscript. This study received grant support from County Council of Stockholm (SLL; ALF 20170480)

Competing interests

The authors declare that they have no conflict of interest.

References

[1] Chinnadurai P, Duran C, Al-Jabbari O et al. Value of C-arm cone beam computed tomography image fusion in maximizing the versatility of endovascular robotics. Ann Vasc Surg 2016; 30: 138–148

[2] de Ledinghen V, Lecesne R, Raymond JM et al. Diagnosis of choledocholithiasis: EUS or magnetic resonance cholangiography? A prospective controlled study Gastrointest Endosc 1999; 49: 26–31

[3] Lee MG, Lee HJ, Kim MH et al. Extrahepatic biliary diseases: 3D MR cholangiopancreatography compared with endoscopic retrograde cholangiopancreatography. Radiology 1997; 202: 663–669

[4] Sandrasegaran K, Lin C, Akisik FM et al. State-of-the-art pancreatic MRI. Am J Roentgenol 2010; 195: 42–53

[5] Adler DG, Baron TH, Davila RE et al. ASGE guideline: the role of ERCP in diseases of the biliary tract and the pancreas. Gastrointest Endosc 2005; 62: 1–8

[6] Andriulli A, Loperfido S, Napolitano G et al. Incidence rates of post-ERCP complications: A systematic survey of prospective studies. Am J Gastroenterol 2007; 102: 1781–1788

[7] Ponchon T, Gagnon P, Berger F et al. Value of endobiliary brush cytology and biopsies for the diagnosis of malignant bile duct stenosis: results of a prospective study. Gastrointest Endosc 1995; 42: 565–572

[8] Liguory C, Gouerou H, Chavy A et al. Endoscopic retrograde cholangiopancreatography. Br J Surg 1974; 61: 359–362

[9] Chandrasekhara V, Khashab MA, Muthusamy VR et al. Adverse events associated with ERCP. Gastrointest Endosc 2017; 85: 32–47

[10] Chang L, Lo SK, Stabile BE et al. Gallstone pancreatitis: a prospective study on the incidence of cholangitis and clinical predictors of retained common bile duct stones. Am J Gastroenterol 1998; 93: 527–531

[11] De Palma GD, Galloro G, Siciliano S et al. Unilateral versus bilateral endoscopic hepatic duct drainage in patients with malignant hilar biliary obstruction: results of a prospective, randomized, and controlled study. Gastrointest Endosc 2001; 53: 547–553

[12] Le Heron J, Padovani R, Smith I et al. Radiation protection of medical staff. European J Radiology 2010; 76: 20–23

[13] Jones DW, Stangenberg L, Swerdlow NJ et al. Image fusion and 3-dimensional roadmapping in endovascular surgery. Ann Vasc Surg 2018; 52: 302–311

[14] McNally MM, Scali ST, Feezor RJ et al. Three-dimensional fusion computed tomography decreases radiation exposure, procedure time, and contrast use during fenestrated endovascular aortic repair. J Vasc Surg 2015; 61: 309–316

[15] Stangenberg L, Shuja F, Carelsen B et al. A novel tool for three-dimensional roadmapping reduces radiation exposure and contrast agent dose in complex endovascular interventions. J Vasc Surg 2015; 62: 448–455

[16] Schwein A, Chinnadurai P, Shah DJ et al. Feasibility of three-dimensional magnetic resonance angiography-fluoroscopy image fusion technique in guiding complex endovascular aortic procedures in patients with renal insufficiency. J Vasc Surg 2017; 65: 1440–1452

[17] Zhang Q, Zhang Z, Yang J et al. CBCT-based 3D MRA and angiographic image fusion and MRA image navigation for neuro interventions. Medicine (Baltimore) 2016; 95: e4358

[18] Lee YN, Moon JH, Choi HJ et al. Tissue acquisition for diagnosis of biliary strictures using peroral cholangioscopy or endoscopic ultrasound-guided fine-needle aspiration. Endoscopy 2019; 51: 50–59

[19] Marya NB, Tabibian JH. Role of endoscopy in the management of primary sclerosing cholangitis. World J Gastrointest Endosc 2019; 11: 84–94

[20] Weigt J, Pech M, Kandulski A et al. Cone-beam computed tomography – adding a new dimension to ERCP. Endoscopy 2015; 47: 654–657

[21] Weigt J, Pech M, Malfertheiner P. Virtual 3D-cholangioscopy: Correlation with direct peroral cholangioscopy in a patient with papillary cholangiocarcinoma. Dig Endosc 2017; 29: 123